A&A 580, L9 (2015)
DOI: 10.1051/0004-6361/201526824

Astronomy & Astrophysics

Letter to the Editor

Wider pulsation instability regions for β Cephei and SPB stars calculated using new Los Alamos opacities

Przemysław Walczak[1], Christopher J. Fontes[2], James Colgan[3], David P. Kilcrease[3], and Joyce A. Guzik[4]

[1] Instytut Astronomiczny Uniwersytet Wrocławski, 51-622 Wrocław, Poland
e-mail: walczak@astro.uni.wroc.pl
[2] Computational Physics Division, Los Alamos National Laboratory, Los Alamos, NM 87545, USA
[3] Theoretical Division, Los Alamos National Laboratory, Los Alamos, NM 87545, USA
[4] Theoretical Design Division, Los Alamos National Laboratory, Los Alamos, NM 87545, USA

Received 24 June 2015 / Accepted 19 July 2015

ABSTRACT

Aims. Our goal is to test the newly developed OPLIB opacity tables from Los Alamos National Laboratory and check their influence on the pulsation properties of B-type stars.
Methods. We calculated models using MESA and Dziembowski codes for stellar evolution and linear, nonadiabatic pulsations, respectively. We derived the instability domains of β Cephei and SPB-types for different opacity tables OPLIB, OP, and OPAL.
Results. The new OPLIB opacities have the highest Rosseland mean opacity coefficient near the so-called Z-bump. Therefore, the OPLIB instability domains are wider than in the case of OP and OPAL data.

Key words. asteroseismology – atomic data – opacity – stars: oscillations

1. Introduction

Radiative opacities are key ingredients in stellar microphysics because they determine the temperature profile within stars. Moreover, the increase in opacity near the so-called Z-bump governs the stellar pulsations of B-type stars (Dziembowski et al. 1993). The commonly used data, such as OP tables from the international Opacity Project (Seaton 2005) and OPAL tables from Lawrence Livermore National Laboratory (Iglesias & Rogers 1996), may be underestimated near the Z-bump. A postulated increase in the opacities can solve some problems in asteroseismic analysis (Pamyatnykh et al. 2004; Zdravkov & Pamyatnykh 2008; Salmon et al. 2012; Walczak et al. 2013; Daszyńska-Daszkiewicz et al. 2013b). Therefore, we tested the new OPLIB opacity tables, which were generated with the ATOMIC code at Los Alamos National Laboratory (Colgan et al. 2013, 2015). We calculated the instability domains of β Cephei and slowly pulsating B-type (SPB) stars. The new opacities are higher near the Z-bump. Therefore, the new instability domains are wider than in the case of OP and OPAL data.

In the next section we briefly summarize the new opacity data. In the following section we discuss new instability domains. The last section contains conclusions.

2. New opacities

As mentioned above, a new set of opacities has been calculated with the Los Alamos suite of modeling codes. OPLIB tables have been generated for the first 30 elements of the periodic table and will soon be available online[1]. This new OPLIB release includes a number of improvements, such as a more accurate equation-of-state treatment and significant fine-structure detail in the atomic physics calculations. For more details, see Colgan et al. (2013, 2015). The opacities used in this work were obtained by mixing the pure-element OPLIB tables under the assumption of electron-temperature and electron-degeneracy equilibrium with the TOPS code[1].

3. Instability domains

One of the most important influences of opacities on stellar models is their impact on pulsational instability. B-type pulsators like β Cep and SPB stars are very suitable for these kinds of studies. Their pulsational behavior is sensitive to the opacity bump caused by iron group elements, mainly Fe (Z-bump). In Fig. 1 we show the Rosseland mean opacity coefficient, κ, plotted as a function of temperature inside of stellar models with effective temperature $\log T_{\rm eff} = 4.187$ and luminosity $\log L/L_{\odot} = 2.976$ (left panel) and $\log T_{\rm eff} = 4.357$ and $\log L/L_{\odot} = 4.028$ (right panel). We assumed the metallicity $Z = 0.015$ and the mixture of the chemical abundances by Asplund et al. (2009, hereafter AGSS09). Different line types indicate different opacity tables: OPAL (solid line), OP (dashed line), and OPLIB (dotted-line). The models are near the middle of the main sequence evolution phase. The masses of models are approximately 5 $M_{\odot}$ (left panel) and 10 $M_{\odot}$ (right panel). The former models can be considered as representative of SPB and the latter for the β Cep stars. The stellar models calculated with different opacities have slightly different masses because we wanted to compare models with the same effective temperature and luminosity. All models were calculated with the MESA evolution code (Paxton et al. 2011, 2013) and the linear nonadiabatic pulsational code of Dziembowski (Dziembowski 1977).

[1] http://aphysics2.lanl.gov/opacity/lanl

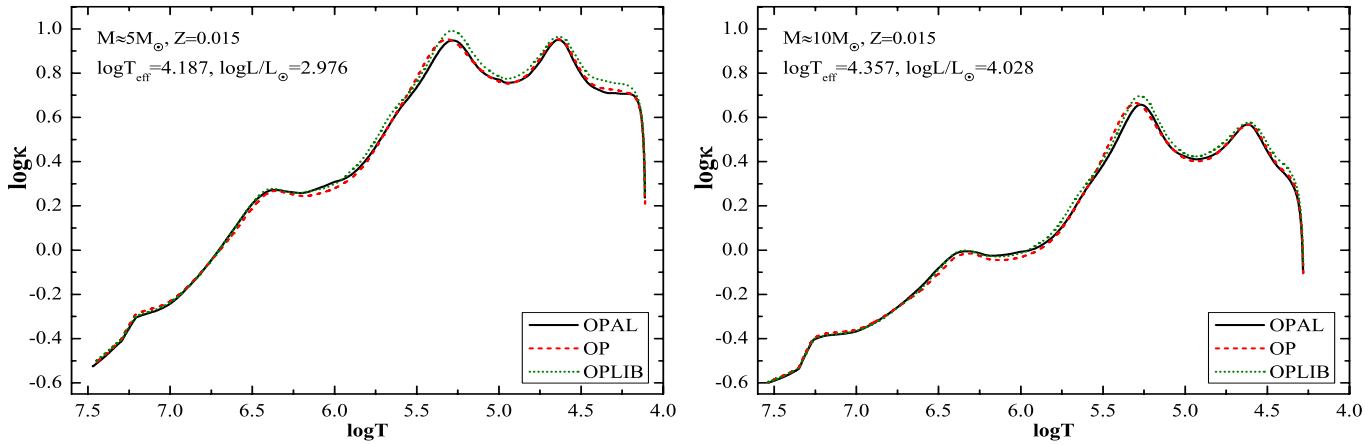

Fig. 1. Comparison of the Rosseland mean opacity coefficient plotted as a function of temperature inside of stellar models with masses of about 5 $M_\odot$ (*left panel*) and 10 $M_\odot$ (*right panel*). We used metallicity $Z = 0.015$ and the element mixture by Asplund et al. (2009). Different lines correspond to different opacity tables (solid line – OPAL, dashed line – OP, and dotted line – OPLIB).

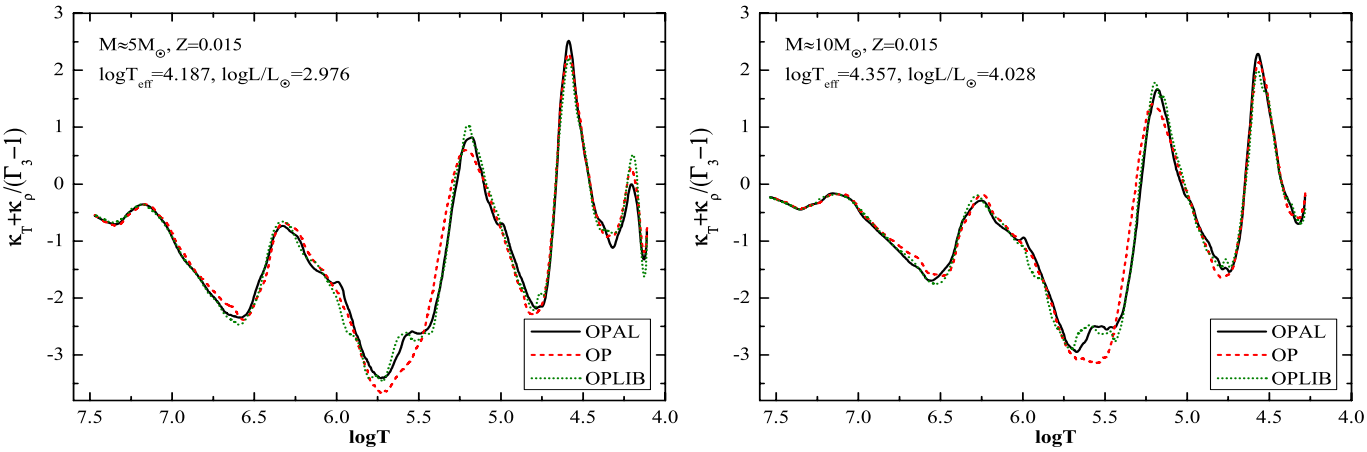

Fig. 2. Same as Fig. 1, but here we show the derivatives of the opacity coefficient. $\kappa_{\rm T}$ and κ_ρ are defined in the text.

In the core of stellar models, there is a jump in the opacity coefficient connected with the transition from convective core to radiative envelope ($\log T \approx 7.25$). The local opacity maximum at $\log T \approx 6.3$ is called the deep opacity bump (DOB), which is due primarily to L-shell bound-free transitions of iron and K-shell bound-free transitions of carbon, oxygen, and neon. At about $\log T = 5.3$, there is the Z-bump, with an increase in opacity caused mainly by M-shell bound-free transitions of iron. The next opacity increase near $\log T = 4.65$ is caused by the second helium ionization.

Near the center of stars, up to $\log T \approx 6.5$, the opacity coefficients are very similar, regardless of the opacity tables. Small differences occur near the DOB. Near the Z-bump, however, we can observe very significant differences in the maximum value of the opacity coefficient. The largest maximum occurs for the new OPLIB opacities. The temperature at the maximum is nearly identical to the case of OPAL data. For OP data the Z-bump occurs at higher temperature, deeper in the star.

The dependence of the OPLIB opacity coefficient on the temperature is similar to the OPAL case, except that the OPLIB coefficient is systematically higher, starting around $\log T = 6.0$. The similar shape gives similar derivatives, which can be noticed in Fig. 2, where we plotted $\kappa_{\rm T} + \kappa_\rho/(\Gamma_3 - 1)$. Here, $\kappa_{\rm T}$ is defined as $\frac{\partial \log \kappa}{\partial \log T}\big|_\rho$, κ_ρ as $\frac{\partial \log \kappa}{\partial \log \rho}\big|_{\rm T}$, and $\Gamma_3 - 1 = \frac{\partial \ln T}{\partial \ln \rho}\big|_{\rm ad}$. The pulsation properties depend directly on this opacity derivative, in particular, the driving of oscillations (Pamyatnykh 1999). For both OPAL and OPLIB tables, we see a local maximum of the derivative near $\log T = 5.6$, which is not present in OP data. Judging by the derivatives, we can expect the main pulsational properties to be similar in the case of OPAL and OPLIB opacities.

In Fig. 3 we present the instability domains in the HR diagram. We also plot the stellar evolution tracks for masses from 2.5 $M_\odot$ up to 30 $M_\odot$. From 2.5 to 15 $M_\odot$, we used a 0.5 $M_\odot$ step. For masses from 15 to 20 $M_\odot$ the step was 1 $M_\odot$, and we used a 2 $M_\odot$ step for masses higher than 20 $M_\odot$. We assumed the chemical mixture AGSS09, metallicity $Z = 0.015$, the initial hydrogen abundance $X = 0.7$, exponential overshooting from the convective core with the overshooting parameter $f = 0.02$ (Herwig 2000), and no rotational velocity. We also marked a part of the blue border of the classical instability strip, where one can find pulsating stars like δ Cephei, RR Lyrae, W Virginis, and δ Scuti.

As seen, the OPLIB opacities give unstable β Cep modes for masses $M > 6$ $M_\odot$, while with the OPAL data we need $M > 6.5$ $M_\odot$. The OPLIB instability also starts much closer to the zero age main sequence (ZAMS). The low-temperature border covers the terminal age main sequence (TAMS) for low-mass stars. The β Cep instability domain reaches the shell hydrogen-burning phase for masses higher than about 13 $M_\odot$ for the OPAL tables and 11.5 $M_\odot$ for the OPLIB data.

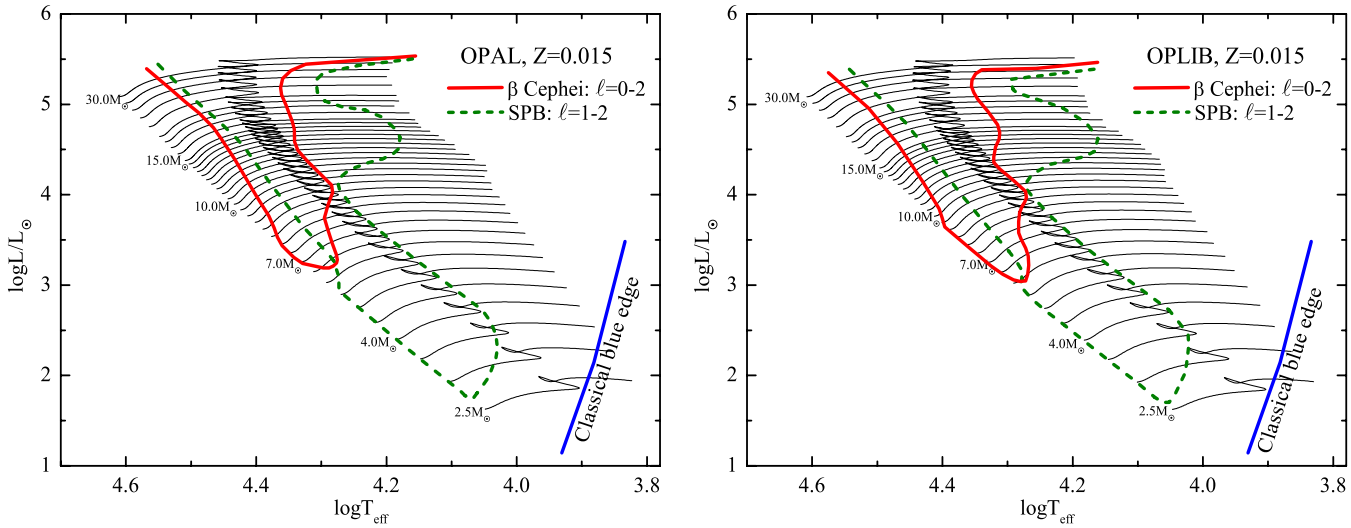

Fig. 3. HR diagram with evolutionary tracks for masses $M = 2.5{-}30\ M_\odot$ and metallicity $Z = 0.015$. The thick solid lines indicate the unstable low-order p- and g-type modes of degrees $\ell = 0{-}2$. Thick dotted lines show the high-order g-mode instability domain. In the *left and right panels*, we assumed the OPAL and OPLIB opacity data, respectively.

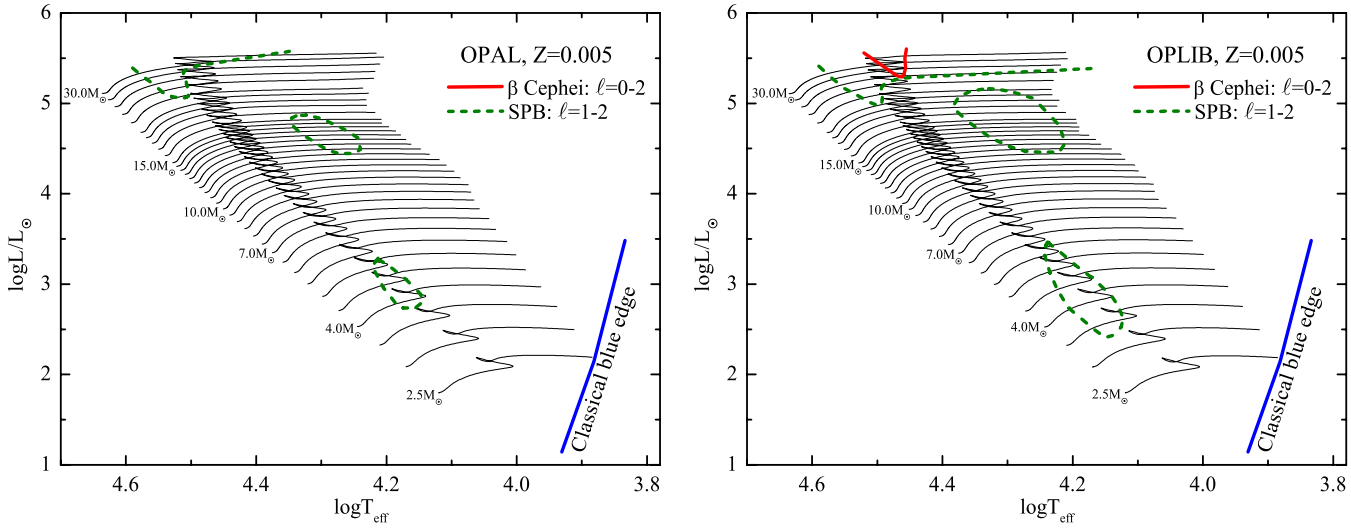

Fig. 4. Same as in Fig. 3, but for $Z = 0.005$.

The high-order g-mode instability strip begins with a mass of about 2.75 $M_\odot$ for both opacity tables. Some small differences can be noticed in the position of the high-temperature border for masses higher than 6 $M_\odot$. In the case of OPLIB tables, this border occurs closer to the ZAMS than in the case of OPAL data. Up to about 10 $M_\odot$, the effective low-temperature border is equal to the TAMS, due to strong damping of the high-order g-modes in the radiative core of the evolved stars (Pamyatnykh 1999). For masses higher than 10 $M_\odot$, the low-temperature border reaches the late post main sequence evolution phase, and it is slightly more extended in the case of the OPLIB opacities. The post-main sequence g-type instability regions are connected with so-called slowly pulsating B-type supergiants (SPBsg). For more detailed discussions on this type of oscillation, see Saio et al. (2006), Godart et al. (2009), Daszyńska-Daszkiewicz et al. (2013a), Ostrowski & Daszyńska-Daszkiewicz (2015).

For lower metallicities, the instability domain starts to disappear. In Fig. 4 we plot the instability domain for metallicity $Z = 0.005$. Now the differences between opacity tables are more significant. For $Z = 0.005$, we do not find any pulsational instability of β Cep type with the OPAL tables. In the case of OPLIB data, there is, however, a small instability domain that covers models near the TAMS with masses higher than 26 $M_\odot$. There were also small SPB instability domains for all opacities. For the OPAL data, they cover the main sequence models with masses from 3.75 $M_\odot$ to 5.25 $M_\odot$ and for $M > 20\ M_\odot$. The SPBsg instability appears for models after main sequence with masses between 11 and 14.5 $M_\odot$. For the OPLIB tables, we have unstable modes for models with masses from 3.25 $M_\odot$ to 6 $M_\odot$ and for masses higher than 20 $M_\odot$. The SPBsg instability domain covers evolved models with masses from 11 to 20 $M_\odot$.

The OP instability domains are somewhat in between the OPAL and OPLIB cases for both β Cep and SPB types of pulsations. The effect of the overshooting efficiency is mainly confined to the location of the TAMS, and it does not significantly influence the instability borders. The blue border of the classical instability strip is nearly insensitive to the opacity tables, as well as to metallicity.

In Fig. 5 we show the instability parameter, η, as a function of the pulsational frequency for selected models. The η parameter measures the net energy gained by a mode during the whole pulsational cycle (Stellingwerf 1978): $\eta = W/\int_0^R |\frac{\mathrm{d}W}{\mathrm{d}r}|\mathrm{d}r$, where W is

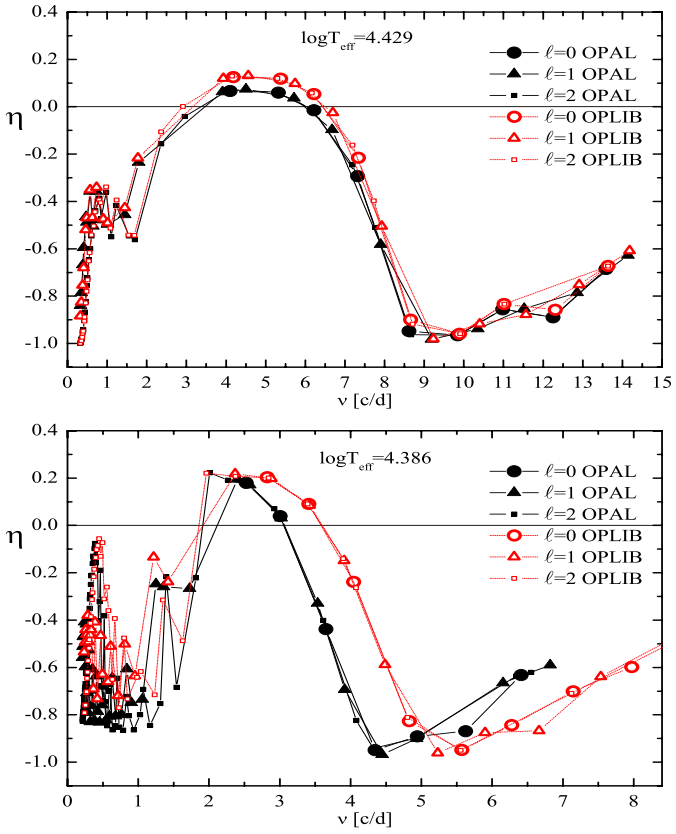

Fig. 5. Instability parameter, η, plotted as a function of frequency (in cycles per day) for $\ell = 0$, 1, 2 modes for models in different evolutionary phases. Solid symbols indicate the OPAL opacities, and empty symbols correspond to the OPLIB data.

the total work integral. For $\eta > 0$, we have unstable modes. We chose models with a mass $M = 15\ M_{\odot}$, metallicity $Z = 0.015$, and two effective temperatures. In the upper panel we have a young model on the main sequence and in the bottom panel a model near the TAMS. A circle indicates radial mode ($\ell = 0$), a triangle indicates dipole mode ($\ell = 1$), and a square indicates a quadrupole mode ($\ell = 2$).

We see that the OPLIB opacities imply instability for higher frequencies, which is clearly visible, especially for the more evolved star model. Also, in many cases, the η-parameter is higher for the OPLIB tables. Relatively small differences occur for low frequencies with $\nu < 2$ cycles per day (c/d).

4. Conclusions

The new OPLIB data have a larger Rosseland mean opacity coefficient than in the case of the OP and OPAL data. The difference between the OPAL and OPLIB data is on the order of 11% for the 5 $M_{\odot}$ model and 9% for the 10 $M_{\odot}$ model. Differences between OP and OPLIB are slightly smaller and are on the order of 9% for the 5 $M_{\odot}$ model and 8% for 10 $M_{\odot}$, therefore the instability domains of B-type pulsators are wider for OPLIB data. The new opacities also influence the pulsational properties of stars, especially the β Cep-type modes, because the higher frequencies are unstable.

Although the changes in opacities went in the right direction, some basic problems of pulsating stars have still not been solved. In general, the new OPLIB opacities cannot explain the pulsations of the B-type stars in the Large Magellanic Cloud (LMC) and the Small Magellanic Cloud (SMC), where many β Cep candidates have been found (Sarro et al. 2009; Pigulski & Kołaczkowski 2002; Kołaczkowski et al. 2006; Diago et al. 2008; Karoff et al. 2008; Pigulski & Pojmański 2008). The metallicity was estimated at $Z \approx 0.005$ for LMC and $Z \approx 0.0025$ for the SMC (Buchler 2008; Salmon et al. 2012). Some β Cep instability can be found with $Z = 0.005$ (see Fig. 4 and Miglio et al. 2007), but for SMC we cannot find any instability of this type. Moreover, there are indications that the theoretical opacities (including OP and OPLIB) are underestimated in the conditions at the base of the solar convection zone, as has been shown through comparison with experiments (Bailey et al. 2015). It seems that the increase in OPLIB opacities is still too small.

In our next papers, we will show the results of more detailed asteroseismic studies of pulsating stars of β Cep/SPB-type: 12 Lacertae and ν Eridani.

Acknowledgements. The research leading to these results has received funding from the European Community's Seventh Framework Program (FP7/2007-2013) under grant agreement No. 269194 and also under the auspices of the US DoE by Los Alamos National Laboratory under Contract No. DE-AC52-06NA25396

References

Asplund, M., Grevesse, N., Sauval, A. J., & Scott, P. 2009, ARA&A, 47, 481
Bailey, J. E., Nagayama, T., Loisel, G. P., et al. 2015, Nature, 517, 56
Buchler, J. R. 2008, ApJ, 680, 1412
Colgan, J., Kilcrease, D. P., Magee, N. H., et al. 2013, High Energy Density Physics, 9, 369
Colgan, J., Kilcrease, D. P., Magee, N. H., et al. 2015, High Energy Density Physics, 14, 33
Daszyńska-Daszkiewicz, J., Ostrowski, J., & Pamyatnykh, A. A. 2013a, MNRAS, 432, 3153
Daszyńska-Daszkiewicz, J., Szewczuk, W., & Walczak, P. 2013b, MNRAS, 431, 3396
Diago, P. D., Gutiérrez-Soto, J., Fabregat, J., & Martayan, C. 2008, A&A, 480, 179
Dziembowski, W. A. 1977, Acta Astron., 27, 203
Dziembowski, W. A., Moskalik, P., & Pamyatnykh, A. A. 1993, MNRAS, 265, 588
Godart, M., Noels, A., Dupret, M. A., & Lebreton, Y. 2009, MNRAS, 396, 1833
Herwig, F. 2000, A&A, 360, 952
Iglesias, C. A., & Rogers, F. J. 1996, ApJ, 464, 943
Karoff, C., Arentoft, T., Glowienka, L., et al. 2008, MNRAS, 386, 1085
Kołaczkowski, Z., Pigulski, A., Soszyński, I., et al. 2006, MmSAI, 77, 336
Miglio, A., Montalbán, J., & Dupret, M. A. 2007, MNRAS, 375, 21
Ostrowski, J., & Daszyńska-Daszkiewicz, J. 2015, MNRAS, 447, 237
Pamyatnykh, A. A. 1999, Acta Astron., 49, 119
Pamyatnykh, A. A., Handler, G., & Dziembowski, W. A. 2004, MNRAS, 350, 1022
Paxton, B., Bildsten, L., Dotter, A., et al. 2011, ApJS, 192, 3
Paxton, B., Cantiello, M., Arras, P., et al. 2013, ApJ, 208, 4
Pigulski, A., & Kołaczkowski, Z. 2002, A&A, 388, 88
Pigulski, A., & Pojmański, G. 2008, A&A, 477, 907
Saio, H., Kuschnig, R., Gautschy, A., et al. 2006, ApJ, 650, 1111
Salmon, S., Montalbán, J., Morel, T., et al. 2012, MNRAS, 422, 3460
Sarro, L. M., Debosscher, J., López, M., & Aerts, C. 2009, A&A, 494, 739
Seaton, M. J. 2005, MNRAS, 362, 1
Stellingwerf, R. F. 1978, AJ, 83, 1184
Walczak, P., Daszyńska-Daszkiewicz, J., Pamyatnykh, A. A., & Zdravkov, T. 2013, MNRAS, 432, 822
Zdravkov, T., & Pamyatnykh, A. A. 2008, Commun. Asteroseismol., 157, 385